

LOW-PRESSURE REVERSIBLE AXIAL FAN DESIGNED WITH DIFFERENT SPECIFIC WORK OF ELEMENTARY STAGES

by

**Božidar P. BOGDANOVIĆ, Živan T. SPASIĆ*, and
Jasmina B. BOGDANOVIĆ-JOVANOVIĆ**

Faculty of Mechanical Engineering, University of Niš, Niš, Serbia

Original scientific paper
DOI: 10.2298/TSCI120503195B

Low-pressure axial fan impellers designed according to the principle of equal specific work of all elementary stages have blades whose profile near the fan hub is under a significantly larger inclination angle than at the impeller periphery. In order to minimize the spatial curvature of the fan blades and the fan hub length, impeller blades of low-pressure axial fans can be designed with different specific work of elementary stages, so that the specific work of elementary stages is smaller at the hub than at the periphery. This paper presents the operating characteristics of a low-pressure reversible axial fan with straight blade profiles, designed with different specific work of elementary stages. The fan was tested on a standard test rig, with air intake loading on the suction side of the fan.

Key words: *reversible axial fan, elementary stages, blade, characteristics, experiment*

Introduction

The basic assumption in the design of axial turbomachinery is that its flow surfaces are axisymmetric. For the flow surfaces to be cylindrical or nearly cylindrical, axial fans are usually designed according to the principle of equal specific work of elementary stages. In order to minimize the spatial curvature of the fan blades and the fan hub length, impeller blades of low-pressure axial fans can be designed with different specific work of elementary stages, so that the specific work of elementary stages is smaller at the hub than at the periphery. For determining the shape of the fan blades it is sufficient to define their profile in 5 to 12 elementary stages, approximately evenly distributed over the height of the blades.

Calculating the fan with different specific work of elementary stages

Figure 1 shows a schematic of a meridian section of a fan impeller, with traces of two elementary immediate axisymmetrical flow surfaces, where one (below) is marked as S_m . A flow space between two elementary immediate axisymmetrical flow surfaces represents an

* Corresponding author; e-mail: zivans@masfak.ni.ac.rs

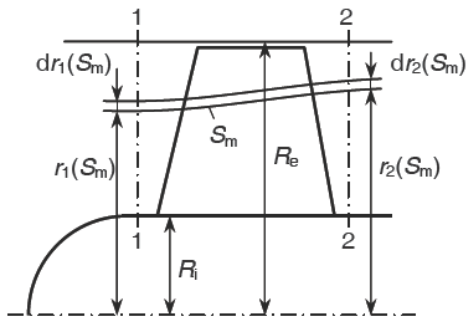


Figure 1. The schematic of a meridian section of a fan impeller; R_i – fan hub radius, R_e – fan periphery radius

elementary stage of the fan runner, and an intersection of axisymmetrical flow surface S_m and fan blades defines the blade profile cascade of the elementary stage.

Control cross-sections in front of (1) and behind (2) the fan impeller are placed far enough from the blade runner, therefore, it can be assumed that flow parameters of the cross-sections do not depend on the circumferential co-ordinate (φ).

For low-pressure axial flow fans that are designed with a fan runner only, the following can be written: $p_{tot1} = \text{const.}$ and $c_{u1} = 0$.

According to the Euler's equations for turbomachinery, the specific work of elementary stage of the fan impeller is:

$$y_k(S_m) = \omega r_2(S_m) c_{u2}(S_m), \quad \text{for } c_{u1} = 0 \quad (1)$$

and the total pressure increase in the elementary stage:

$$\Delta p_{tot}(S_m) = p_{tot2}(S_m) - p_{tot1}(S_m) = p_{tot2}[r_2(S_m)] - p_{tot1} \quad (2)$$

or

$$\Delta p_{tot}(S_m) = \eta_h(S_m) \rho y_k(S_m) \quad (3)$$

where $\eta_h(S_m)$ is the hydraulic efficiency of elementary stage if the fan impeller:

$$\eta_h(S_m) = \frac{\Delta p_{tot}(S_m)}{\rho y_k(S_m)} = 1 - \frac{\Delta y_g(S_m)}{y_k(S_m)} \quad (4)$$

where $\Delta y_g(S_m)$ is the mechanical loss of flow energy in the elementary stage of the fan impeller.

It is assumed that the hydraulic efficiency is equal for all elementary stages.

If $Q[r(S_m)]$ is the flow rate of the gas flowing through the flow space between the fan hub and the axisymmetrical flow surface S_m , according to the continuity law (for $\rho_1 = \rho_2 = \rho = \text{const.}$), follows:

$$Q[r(S_m)] = 2\pi \int_{R_i}^{r_1(S_m)} c_{z1}(r) r dr = 2\pi \int_{R_i}^{r_2(S_m)} c_{z2}(r) r dr \quad (5)$$

where c_{z1} and c_{z2} are the distribution functions of axial component of flow velocity in control cross-sections in front of and behind the fan impeller, which have to fulfill the requirement:

$$Q = 2\pi \int_{R_i}^{R_e} c_{z1}(r) r dr = 2\pi \int_{R_i}^{R_e} c_{z2}(r) r dr \quad (6)$$

For the known function $y_k(r)$, the specific work of the fan impeller can be calculated using the equation:

$$Y_k = \frac{1}{Q} \int_{A_2} y_k(r) \cdot dQ = \frac{1}{Q} \left[2\pi \int_{R_i}^{R_e} y_k(r) \cdot c_{z_2}(r) \cdot r dr \right] \quad (7)$$

The necessary condition is that control cross-sections are placed in the space which is physically bounded by the cylindrical surface of the fan hub ($R_i = \text{const.}$) and the fan shroud ($R_e = \text{const.}$).

The equation of steady fluid flow of the inviscous fluid can be written in the form: (for cylindrical flow surfaces the flow does not depend on the circumferential co-ordinate (φ)).

$$c_z \frac{\partial c_z}{\partial r} + \frac{c_u}{r} \frac{\partial (rc_u)}{\partial r} = \frac{1}{\rho} \frac{\partial p_{\text{tot}}}{\partial r} \quad (8)$$

For the fluid flow in front of the fan impeller $c_u = c_{u1} = 0$ and $p_{\text{tot}} = p_{\text{tot1}} = \text{const.}$, therefore due to eq. (8), for $c_z = c_{z1}$, follows: $\partial c_{z1}/\partial r = 0$, tj. *i. e.* $c_{z1} = \text{const.}$

The total pressure in the control cross-section 2 of the fan impeller $\eta_h(S_m) = \text{const.}$, $p_{\text{tot1}} = \text{const.}$ and $y_k(S_m) = y_k(r)_2$ is:

$$p_{\text{tot}_2}(r) = p_{\text{tot}_1} + \rho \eta_h Y_k(r)_2 \quad (9)$$

and circumferential component of absolute velocity:

$$rc_{u_2} = \frac{1}{\omega} y_k(r)_2 \quad \text{and} \quad c_{u_2} = \frac{1}{r\omega} y_k(r)_2 \quad (10)$$

Considering the above equations for obtaining cylindrical surfaces in the control cross-sections behind the fan impeller (for $p_{\text{tot}} = p_{\text{tot2}}$; $c_z = c_{z2}$, and $c_u = c_{u2}$), the following is assumed:

$$c_{z_2} \frac{\partial c_{z_2}}{\partial r} = \left[\eta_h - \frac{1}{r^2 \omega^2} y_k(r) \right] \frac{\partial y_k(r)}{\partial r} \quad (11)$$

where

$$\eta_h - \frac{1}{r^2 \omega^2} y_k(r) > 0$$

By analyzing this equation, one can conclude:

- the flow surfaces in fan impeller are cylindrical, for $Y_k(r) = \text{const.}$; $\partial y_k(r)/\partial r = 0$, $c_{z2} = c_{z1} = \text{const.}$, $\Rightarrow r_2(S_m) = r_1(S_m)$, and
- cylindrical flow surfaces in the control cross-sections in front of and behind the fan runner do not remain cylindrical inside the fan impeller: $\partial y_k(r)/\partial r > 0$, $\partial c_{z2}/\partial r > 0$, $\Rightarrow r_2(S_m) > r_1(S_m)$.

Distribution function of specific work of elementary stages

In order to reduce the specific work of elementary stages near the fan hub, and for flow surfaces inside the fan runner not to deviate much from the cylindrical surfaces, the distribution function of specific work of elementary stages is suggested [1, 2]:

$$\left. \begin{aligned} y_k(r) &= A + 2r_0Br - Br^2, \quad \text{za } R_i \leq r \leq r_0 \\ y_k(r) &= y_{k.o} = \text{const.}, \quad \text{za } r_0 \leq r \leq R_e \end{aligned} \right\} \quad (12)$$

where $\partial y_k(r)/\partial r = 0$, for $r = r_0$.

The function $y_k(r)$ is defined according to assumption parameters r_0 ($R_i \leq r_0 \leq R_e$) and $y_{k.i} = y_k(R_i)$, and the recommendation is:

$$r_0 \leq \frac{1}{2}(R_i + R_e) \quad \text{and} \quad y_{k.i} = (0,6 - 0,7)Y_k^+ \quad (13)$$

where Y_k^+ is the calculation of the (nominal) specific work of the fan impeller.

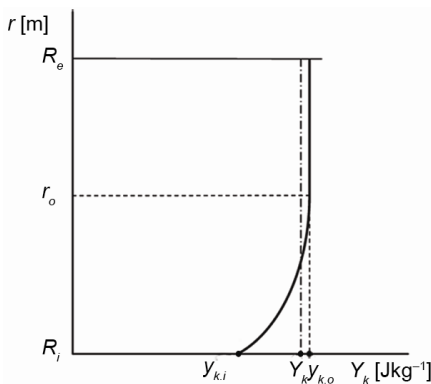


Figure 2. The graph of the function $y_k(r)$

The graph of the function $y_k(r)$, defined by eq. (12), is shown in fig. 2.

The value of the specific work $y_{k.o}$ is unknown, and it can be determined according to the requirement that the specific work obtained by eq. (7) is equal to the nominal specific work of the fan impeller ($Y_k = Y_k^+$).

The value $y_{k.o}$ is obtained by the iterative procedure. In the iterative procedure of the determination of $y_{k.o}$, that is, $y_k(r)$, coefficients A and B existing in the first expression of eq. (12) can be calculated using the following equation obtained from the requirement that $y_k(R_i) = y_{k.i}$ for $r = R_i$ and $y_k(r_0) = y_{k.o}$ for $r = r_0$:

$$B = \frac{y_{k.o} - y_{k.i}}{(r_0 - R_i)^2}, \quad A = y_{k.o} - r_0^2 B \quad (14)$$

Assuming that the flow surfaces are cylindrical in the control cross-section behind the fan impeller, the following is obtained:

$$\left. \begin{aligned} \frac{\partial c_{z_2}^2}{\partial r} &= \alpha - \beta r + \frac{\gamma}{r} - \frac{\delta}{r^2}, \quad \text{za } R_i \leq r \leq r_0 \\ c_{z_2} &= \text{const.} = c_{z_2}(0), \quad \text{za } r_0 \leq r \leq R_e \end{aligned} \right\} \quad (15)$$

where

$$\begin{aligned} \alpha &= 4r_0 B \left(\eta_h + \frac{3B}{\omega^2} \right), \quad \beta = 4B \left(\eta_h + \frac{B}{\omega^2} \right), \\ \gamma &= 4B \frac{A - 2r_0^2 B}{\omega^2}, \quad \delta = \frac{4r_0 AB}{\omega^2} \end{aligned} \quad (16)$$

By integrating the first expression of eq. (15), the following is obtained:

$$c_{z_2}(r) = \sqrt{\left[c_{z_2}(0) \right]^2 - \alpha(r_0 - r) + \frac{1}{2}\beta(r_0^2 - r^2) - \gamma \ln \frac{r_0}{r} + \delta \left(\frac{1}{r} - \frac{1}{r_0} \right)} \quad (17)$$

The equations used in the iterative procedure of the determination of $y_{k,0}$ and $c_{z2}(0)$, taking into account the form of functions $c_{z2}(r)$ and $y_k(r)$, are derived in the following forms:

$$Q = 2\pi \int_{R_i}^{r_0} c_{z2}(r) r dr + \pi c_{z_2}(0) (R_e^2 - r_0^2) \quad (18)$$

$$Y_k = \frac{1}{Q} 2\pi \int_{R_i}^{r_0} y_k(r) c_{z_2}(r) r dr + \frac{1}{Q} \left[\pi y_{k,0} c_{z_2}(0) (R_e^2 - r_0^2) \right] \quad (19)$$

Values $y_{k,0}$ and $c_{z2}(0)$ are determined by the iterative procedure, using the programs [1]. Apart from determining the values $y_{k,0}$ and $c_{z2}(0)$, the program is created in such a way so as to also yield $y_k(r)$, $c_{z2}(r)$ and $Q(r)$ in the defined step, where r is the radius in control cross-section behind the fan impeller and $Q(r)$ is the flow rate under the cylindrical flow surface of the radius r .

According to the data for $Q(r)$, a functional relation of cylindrical axisymmetrical flow surface radius in front of and behind the fan impeller can be established. Due to eq. (5), for $Q[r(S_m)] = Q(r)$, $r_1(S_m) = r_1(r)$, and $c_{z1} = \text{const.} = c_{zsr}$, the following is obtained:

$$r_1(r) = \sqrt{R_i^2 + \frac{Q(r)}{\pi c_{sr}(z)}} \quad (20)$$

According to the relation $r/r_1(r)$, a deviation between axisymmetrical and cylindrical flow surfaces can be evaluated.

In references [1-3], fan impeller blades are designed for the assumed value of specific work of elementary stages at the hub $y_{k,i}$ ($y_{k,i} = 0,6Y_k^+$) and different values of radius r_0 where one can observe the change in the spatial curvature of the fan blades $\Delta\beta_L = \Delta\beta_i = \beta_{ii} - \beta_{ie}$ and profile cascade width for elementary stages, especially at the fan hub (b_i) which defines the minimum length of the hub.

Calculation of the model fan

For calculation parameters: $Q^+ = 3.61 \text{ m}^3/\text{s}$, $\Delta p_{\text{tot}}^+ = 180 \text{ Pa}$, $n = 1405 \text{ rpm}$ ($Y_k^+ = 200 \text{ J/kg}$, $c_{zsr} = 15.73 \text{ m/s}$) for assumed efficiency (hydraulic $\eta_h = 0.75$ and total $\eta = 0.65$), according to the model with constant specific work of elementary stages, a fan with the geometry of the impeller was designed [2-4]:

- $R_i = 0.150 \text{ m}$ – radius of the fan impeller hub,
- $R_e = 0.315 \text{ m}$ – peripheral radius of the fan impeller, and
- $z_K = 6$ – number of impeller blades.

For the given calculation parameters and with equal blade profile lengths l for elementary stages i (tab. 1), the calculation of the axial fan impeller with different specific work of elementary stages was performed. The calculation was performed according to the model where specific work of elementary stages changed along the entire height of the blade ($r_0 = R_e$) as in the extreme case [1].

For $r_0 = R_e = 0,315 \text{ m}$ and $y_{k,i} = 0,6Y_K = 120 \text{ J/kg}$ the function of the change of specific work along radius r is obtained:

$$y_k(r) = -164.13 + 2486.1 r - 3946 r^2, \quad (21)$$

and the function of the change of velocity:

$$c_{z_2}(r) = \sqrt{A_r + 692 \ln \frac{0,315}{r} - 37,8 \left(\frac{1}{r} - 3,175 \right)} \tag{22}$$

$$A_r = 16,82^2 - 6453(0,315 - r) + 7360(0,0992 - r^2)$$

where values for $r = r_0$ are given in fig. 3.

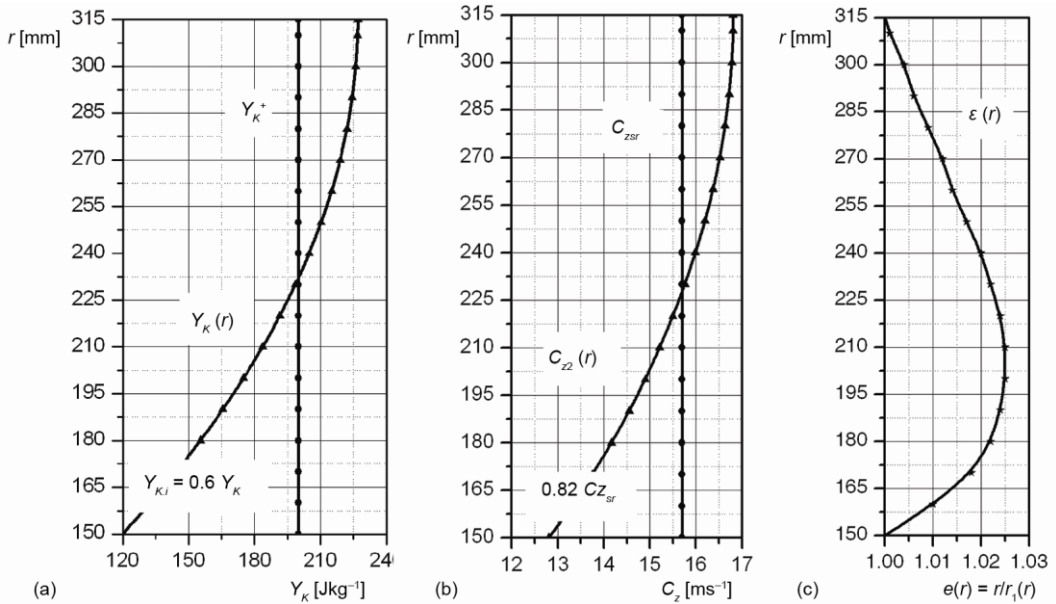


Figure 3. Graphs of the functions; (a) $y_k(r)$, (b) $c_{z_2}(r)$, and (c) $\varepsilon(r)$

For calculation operating parameters, according to which the graphs of the functions of specific work $y_k(r)$, fig. 3(a), and meridian component of absolute velocity $c_{z_2}(r)$, fig. 3(b), were determined, a low-pressure reversible axial fan with straight blade profiles was constructed.

Table 1. Results of the calculations

Section i	r_i [mm]	t_i [mm]	l_i [mm]	t_i/l_i [-]	β_{ti} [°]
I	150	157	144	1.09	41.5
II	178	186	138	1.35	37.9
III	205	215	133	1.61	34.7
IV	233	243	126	1.93	32.6
V	260	272	121	2.25	30.4
VI	288	301	114	2.64	28.3
VII	315	330	108	3.05	26.4

Maximum deviation between axisymmetrical and cylindrical flow surfaces was 2.6%, fig. 3(c), therefore the calculation was performed using the model of cylindrical flow surfaces and taking into account the velocity distribution $c_{z_2}(r)$ and using the method of lift forces. The results of the calculations [2] are given in tab. 1.

The difference in the inclination angles of the profile mean line at the hub of the profile ($\beta_{ti} = 41.5^\circ$) and the shroud ($\beta_{te} = 26.4^\circ$), the angular spatial blade curvature $\Delta\beta_L$ (tab. 1 and fig. 3), is $\Delta\beta_L = \Delta\beta_i = \beta_{ti} - \beta_{te} = 41.5 - 26.4 = 15.1^\circ$, with the profile cascade width of $b_i = 95.4$ mm.

The fan impeller blade designed according to the unequal distribution of specific work of the elementary stages (fig. 4), has a smaller spatial curvature than the fan blade constructed

according to the equal distribution of specific work of all elementary stages by 14° [2, 3]. The inclination angles of the profile mean line at the hub are smaller, that is, a smaller profile cascade width at the hub by 21 mm (22%) which requires the smaller length of the hub impeller [2].

Manufacture of the model for experimental testing

Based on the calculation of the fan, for seven equally distributed elementary stages along the height of the impeller blade (tab. 1), a blade with straight profiles was designed (PP2 profiles) [2]. On the basis of the defined profiles for seven elementary stages, a 3-D blade was designed in the SolidWorks program, which could serve as a model to obtain the geometry of the blade profile for any cylindrical section along the height of the blade. This fact was used in the manufacturing of the blade model from segments.

The blade model (fig. 5) was manufactured from thin stacked and glued straight profile wooden segments (26 segments), whose drawings were prepared and done in SolidWorks. After gluing the segments together, the surface of the blades was planed.

To determine the accurate geometry of the blade model, scanning was performed on a 3-D scanner type MDX-20 (fig. 6), with the scanning step of 0.05 mm in the direction of axes x and y, and in the direction of axis z with the step of 0.025 mm.

Following the spatial scanning of the blade, the 3-D geometry of the blade was obtained, and it was possible to create cylindrical sections of the blade in SolidWorks, so as to obtain the geometry and inclination of blade profiles (2-D) in cylindrical sections (tab. 2). Figure 7 shows the profile mean lines of the scanned blade developed in a plane.

The scanned model of the fan blade has a spatial curvature which is defined as a difference between the inclination angles at the hub and the shroud, $\Delta\beta_L = \Delta\beta_t = \beta_{ti} - \beta_{te} = 12^\circ$ (fig. 7). The model has a smaller spatial curvature in relation to the designed blade by 3.1° , which is explained by the error in the described technology for model manufacturing.

The scanned model of the blade with a straight profile has a smaller spatial curvature than the model of the blade designed with equal specific work of elementary stages ($\Delta\beta_L = \Delta\beta_t = \beta_{ti} - \beta_{te} = 29.1^\circ$) by 17.1° [2].

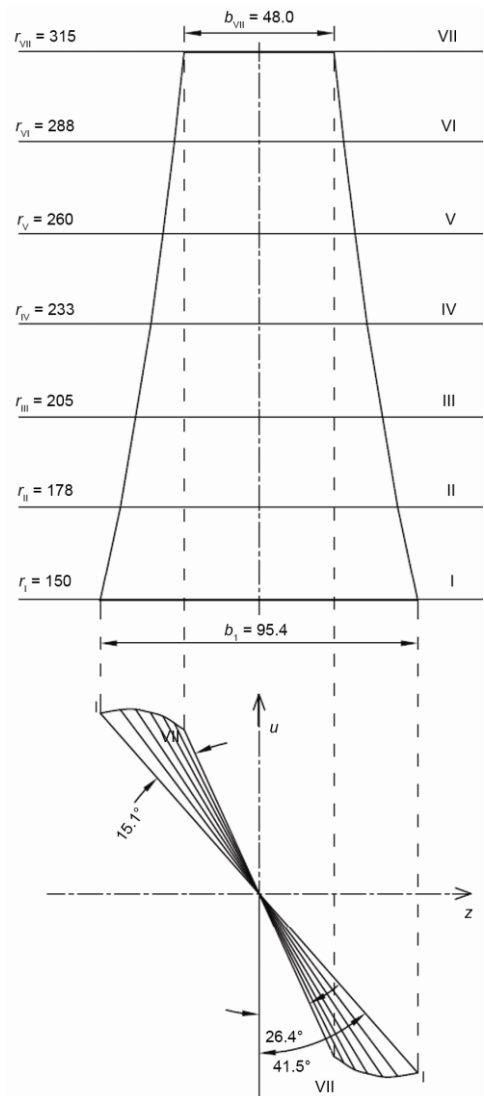


Figure 4. Blade with profile mean lines developed in a plane, $\Delta\beta_L = 15.1^\circ$

the geometry and inclination of blade profiles

(2-D) in cylindrical sections (tab. 2). Figure 7 shows the profile mean lines of the scanned blade developed in a plane.

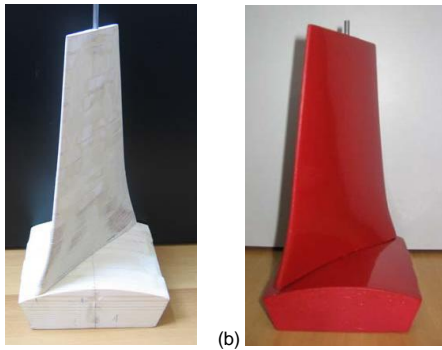


Figure 5. Blade model manufactured from wooden segments; (a) before painting, (b) after painting

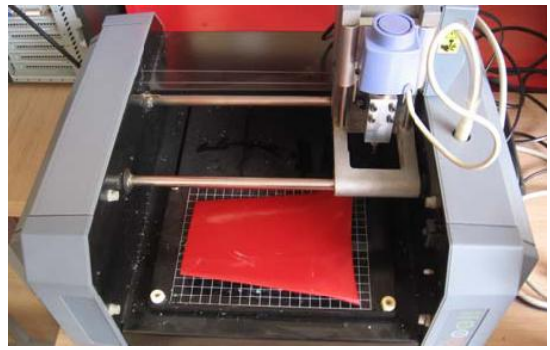


Figure 6. Scanning the model blade on the MDX-20 scanner

Table 2. Dimensions of the scanned blade

Section i	r_i [mm]	h_i [mm]	h_i/h [-]	l_i [mm]	$\Delta\beta_{ii}$ [°]	δ_{maxi} [mm]	$r_{1,2}$ [mm]	$(\delta_{max}/l)_i$ [-]
I	150	0	0.0000	144.0	12	12.0	2.40	0.08
II	160	10	0.0606	141.6	9.6	11.6	2.32	0.08
III	170	20	0.1212	139.1	7.5	11.3	2.26	0.08
IV	180	30	0.1818	137.6	6.5	10.9	2.18	0.08
V	190	40	0.2424	135.6	5.0	10.5	2.10	0.08
VI	200	50	0.3030	132.7	4.3	10.2	2.04	0.08
VII	210	60	0.3636	130.7	3.8	9.8	1.96	0.07
VIII	220	70	0.4242	128.7	3.2	9.5	1.90	0.07
IX	230	80	0.4848	126.2	2.9	9.1	1.82	0.07
X	240	90	0.5455	123.8	2.6	8.7	1.74	0.07
XI	250	100	0.6061	121.3	2.1	8.4	1.68	0.07
XII	270	120	0.7273	117.3	1.5	7.6	1.52	0.06
XIII	290	140	0.8485	113.9	1.0	6.9	1.38	0.06
XIV	310	160	0.9697	109.9	0.6	6.3	1.26	0.06
XV	315	165	1.0000	107.9	0	6.2	1.24	0.06

Table 2 key: i – cylindrical section, r_i – radius, h_i – height of the blade up to the cylindrical section, h_i/h – relative height of the blade, l_i – the length of the blade profile mean line, $\Delta\beta_{ii}$ – difference between the profile mean line inclination angles in the specific cylindrical section and the peripheral section, δ_{maxi} – maximum thickness of blade profile, $r_{1,2}$ – radii of the rounding of the blade profile end, δ_{max}/l_i – relative maximum thickness of the blade profile

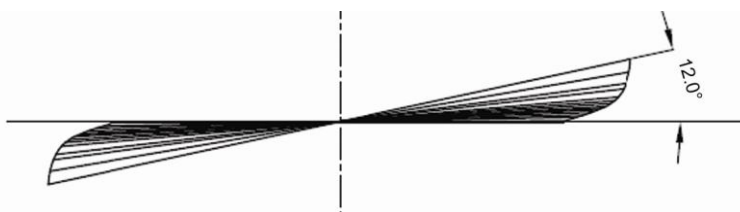


Figure 7. Profile mean lines of the scanned blade developed in a plane, $\Delta\beta_L = 12^\circ$

Experimental testing

The testing and obtaining of the operating characteristics of the fan was conducted by air loading on the suction side of the fan, for a nominal rotation speed of the electric motor $n = 1405$ rpm [5, 6]. The diameter of the fan shroud was $D_e' = 635$ mm, the periphery diameter of the impeller was $D_e = 630$ mm and the diameter of the impeller hub was $D_i = 300$ mm.

The testing was conducted on a standard test rig (AMCA 210), with the suction duct with the diameter $D = 690$ mm (fig. 8), in the Laboratory for Hydraulic and Pneumatic Testing of the Faculty of Mechanical Engineering in Nis. Apart from measuring the pressure and determining the flow, the electrical magnitudes at the entry into the electric motor of the fan, and the rotation speed of the fan and air parameters in the laboratory (atmospheric pressure and temperature) were also measured. The power of the electric motor was $P_M = 1.5$ kW, the characteristics of which were known [2].

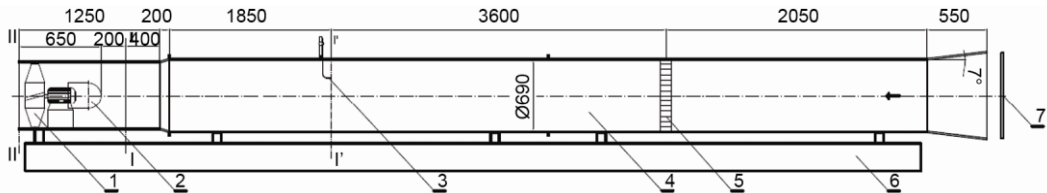


Figure 8. Test rig for testing axial flow fans

1 – Fan for testing, 2 – Deflector, 3 – Prandtl probe with traverse, 4 – Channel testing, 5 – Airflow straightener, 6 – Stand, I'-I' – Cross-section for measuring flow rate, I-I – Cross-section in front of the fan, II-II – Cross-section behind the fan

The volume flow rate was determined on the basis of the measured and mean pressure rate in the cross section I'-I'. The dynamic pressure was measured with the Prandtl probe in five points that were deployed on the defined radii [2, 6]. The total rise in the pressure in the fan was determined as the difference of total pressures behind (p_{IItot}) and in front of the fan (p_{IItot}):

$$\Delta p_{tot} = p_{IItot} - p_{IItot} \quad (23)$$

For testing the fan for suction and free airflow outlet into the atmosphere (fig. 8), the total rise in the pressure in the fan equaled the static pressure (vacuum) in the cross-section in front of the fan [4]:

$$\Delta p_{tot} = p_1^{(v)} \quad (24)$$

Static pressure in front of the fan was measured in the cross section I-I, using a piezometer ring, while static pressure behind the fan (cross section II-II) was considered as equal to the atmospheric pressure.

Results of the experimental testing

The model of the fan was tested for five positions of the impeller blade angle (β_L) measured at the hub: $\beta_L = 40^\circ$, $\beta_L = 42.5^\circ$, $\beta_L = 45^\circ$, $\beta_L = 47.5^\circ$, and $\beta_L = 50^\circ$. The clearance which appeared between the blade and the hub upon the rotation of the blade due to the cylin-

drical shape of the hub, was filled with silicone. For the region of the stable performance of the fan, the diagrams of operating characteristics of the fan are shown, total pressure rise $\Delta p_{\text{tot}}(Q)$, power $P(Q)$ and efficiency $\eta(Q)$, obtained on the testing stand for various impeller blades angle (β_L). The fan characteristics were calculated for a constant rotation speed of the fan $n = 1405$ rpm and air density $\rho = 1.2$ kg/m³.

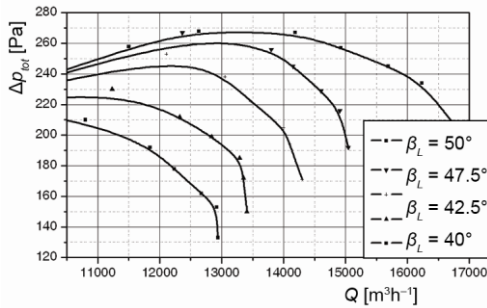


Figure 9. Total pressure rise of the fan, $\Delta p_{\text{tot}}(Q)$

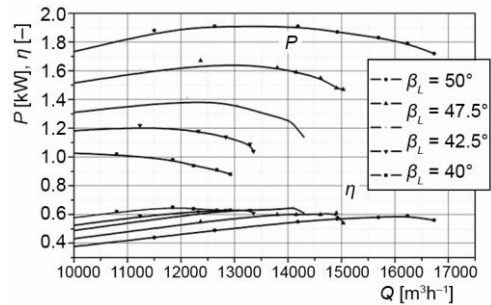


Figure 10. Power and efficiency characteristics, $P(Q)$ and $\eta(Q)$

The analysis of the obtained results: calculation parameters ($\Delta p_{\text{tot}} = 180$ Pa, $Q = 3.61$ m³/s = 13000 m³/h), for the nominal rotation speed of the electric motor ($n = 1405$ rpm) were achieved for the impeller blade angle of $\beta_L = 41.5^\circ$, with relatively high efficiency $\eta = 0.64$.

In optimal operating regime ($\eta = \eta_{\text{max}}$), the fan achieved a maximum efficiency of $\eta = 0.64$ ($\Delta p_{\text{tot}} = 185$ Pa, $Q = 12000$ m³/h) for the impeller blade angle of $\beta_L = 40^\circ$. With the increase of the blade angle, the fan flow and total pressure rise increase too, but the values of efficiency decreased. For the impeller blade angle $\beta_L = 50^\circ$ ($\Delta p_{\text{tot}} = 235$ Pa, $Q = 16200$ m³/h), the efficiency was $\eta = 0.59$.

Conclusions

The reversible axial fan with straight blade profiles designed according to the model with different specific work of elementary stages has the angular spatial curvature smaller by 17.1° and the width of the blade profile cascade at the hub smaller by 20.6 mm (22%), which requires a smaller length of the impeller hub in relation to the blades designed according to the model with the constant specific work of elementary stages [2].

The blades of the fan impeller designed according to the model of unequal specific work of elementary stages, due to the smaller width of the profile cascade at the hub, require a smaller length of the hub, are easier to manufacture, and have slightly lower efficiency than the blades designed with the constant specific work of elementary stages [2].

On the basis of the conducted testing, it is suggested that the design of low-pressure reversible axial fans be performed according to the model with unequal specific work of elementary stages.

Nomenclature

c_z – axial velocity component, [ms⁻¹]
 l – profile length, [m]
 n – rotation speed, [rpm]

P – power, [W]
 p – pressure, [Pa]
 Δp_{tot} – total pressure rise, [Pa]

Q – flow rate of the fan, [$\text{m}^3 \text{s}^{-1}$]
 r – radius, [m]
 t – pitch, [m]
 Y_K – specific work of the impeller, [Jkg^{-1}]
 $y_k(r)$ – specific work of elem. stage, [Jkg^{-1}]

Greek symbols

β_L – impeller blade angle, [$^\circ$]
 β_k – angle inclination of the profile mean line, [$^\circ$]
 δ – thickness profile, [m]

$\Delta\beta_L$ – spatial curvature of the blade, [$^\circ$]
 η – efficiency, [-]
 ρ – density, [kgm^{-3}]

Subscripts

1, 2 – inlet and outlet
t – mean line
e – periphery
i – for hub, cylindrical sections
h – hydraulic
k – impeller

References

- [1] Bogdanović, B., Bogdanović-Jovanović, J., Spasić, Ž., Designing of Low Pressure Axial Flow Fans with Different Specific Work of Elementary Stages, *Proceedings on CD*, The international conference Mechanical Engineering in XXI Century, 2011, Faculty of Mechanical Engineering, University of Nis, Nis, Serbia, pp. 99-102
- [2] Spasić, Ž., Numerical and Experimental Investigation of the Influence of the Blade Profile Shape on the Reversible Axial Fan Characteristics (in Serbian), Ph. D. thesis, Faculty of Mechanical Engineering, University of Nis, Nis, Serbia, 2012
- [3] Bogdanović, B., et al., *The Development Construction of Reversible Axial Fans* (in Serbian), Report for project No. 18012, funded by the Serbian Ministry of Education, Science and Technological Development, the period: 31.04.2008-31.04.2011
- [4] Eck, B., *Fans-Design and Operation of Centrifugal, Axial-Flow and Cross-Flow Fans*, Pergamont Press, Oxford, England, 1973
- [5] Spasić, Ž., Bogdanović, B., Radić, M., Variation of Operation of Low-Pressure Reversible Axial Fans Driven by Induction Motor from Start to the Steady-State, *Proceedings on CD*, SIMTERM 2011, Sokobanja, 2011, pp. 586-595
- [6] Bogdanović, B., Milenković, D., Bogdanović-Jovanović, J., Fans-Performance and Operating Characteristics (in Serbian), Faculty of Mechanical Engineering, University of Nis, Nis, Serbia, 2012